1-1-2005

Atomic layer depostion of TiO2/Al2O3 films for optical applications

G Triani
Australian Nuclear Science and Technology Organisation

P J. Evans
Australian Nuclear Science and Technology Organisation

D RG Mitchell
Australian Nuclear Science and Technology Organisation, dmitchel@uow.edu.au

D J. Attard
Australian Nuclear Science and Technology Organisation, darrena@uow.edu.au

K Finnie
Australian Nuclear Science and Technology Organisation

See next page for additional authors

Atomic layer depostion of TiO2/Al2O3 films for optical applications

Abstract

Atomic layer deposition (ALD) is an important technology for depositing functional coatings on accessible, reactive surfaces with precise control of thickness and nanostructure. Unlike conventional chemical vapour deposition, where growth rate is dependent on reactant flux, ALD employs sequential surface chemical reactions to saturate a surface with a (sub-) monolayer of reactive compounds such as metal alkoxides or covalent halides, followed by reaction with a second compound such as water to deposit coatings layer-by-layer. A judicious choice of reactants and processing conditions ensures that the reactions are self-limiting, resulting in controlled film growth with excellent conformality to the substrate.

This paper investigates the deposition and characterisation of multi-layer TiO2 /Al2O3 films on a range of substrates, including silicon , soda glass and polycarbonate, using titanium tetrachloride/water and trimethylaluminium/water as precursor couples. Structure-property correlations were established using a suite of analytical tools, including transmission electron microscopy (TEM), secondary ion mass spectrometry (SIMS), X-ray reflectometry (XRR) and spectroscopic ellipsometry (SE). The evolution of nanostructure and composition of multi-layer high/low refractive index stacks are discussed as a function of deposition parameters.

Keywords

optical, films, al2o3, tio2, depostion, layer, applications, atomic

Disciplines

Engineering | Physical Sciences and Mathematics

Publication Details

Triani, G., Evans, P. J., Mitchell, D. RG., Attard, D. J., Finnie, K., James, M., Hanley, T., Latella, B., Prince, K. and Bartlett, J. (2005). Atomic layer depostion of TiO2/Al2O3 films for optical applications. SPIE Conference on Optics and Photonics

Authors

G Triani, P J. Evans, D RG Mitchell, D J. Attard, K Finnie, M James, T Hanley, B Latella, Kathryn Prince, and J Bartlett

Atomic Layer Deposition of TiO_2 / Al_2O_3 Films

For Optical Applications

Gerry Triani *, Peter J. Evans, David R.G. Mitchell, Darren J. Attard,
Kim S. Finnie, Michael James, Tracey Hanley, Bruno Latella,
Kathryn E. Prince and John Bartlett

Australian Nuclear Science and Technology Organisation
PMB1, Menai NSW 2234, Australia.

ABSTRACT

Atomic layer deposition (ALD) is an important technology for depositing functional coatings on accessible, reactive surfaces with precise control of thickness and nanostructure. Unlike conventional chemical vapour deposition, where growth rate is dependent on reactant flux, ALD employs sequential surface chemical reactions to saturate a surface with a (sub-) monolayer of reactive compounds such as metal alkoxides or covalent halides, followed by reaction with a second compound such as water to deposit coatings layer-by-layer. A judicious choice of reactants and processing conditions ensures that the reactions are self-limiting, resulting in controlled film growth with excellent conformality to the substrate.

This paper investigates the deposition and characterisation of multi-layer TiO_2 /Al_2O_3 films on a range of substrates, including silicon <100>, soda glass and polycarbonate, using titanium tetrachloride/water and trimethylaluminium/water as precursor couples. Structure-property correlations were established using a suite of analytical tools, including transmission electron microscopy (TEM), secondary ion mass spectrometry (SIMS), X-ray reflectometry (XRR) and spectroscopic ellipsometry (SE). The evolution of nanostructure and composition of multi-layer high/low refractive index stacks are discussed as a function of deposition parameters.

Keywords: Atomic layer deposition, alumina, titania, multi-layer coatings, TEM, SIMS, XRR, ellipsometry

1. INTRODUCTION

Atomic layer deposition (ALD) is an enabling technology that is currently being investigated in the scale-down of integrated circuits for the semiconductor industry. Originally conceived as a method for depositing both polycrystalline ZnS and amorphous dielectric thin films for electroluminescent flat panel displays [1]. The applications base of ALD has extended because of its ability to produce uniform high-quality, pinhole-free films over large areas. ALD films can now be found in magnetic recording heads [2], as protective coatings in photonics packages [3], and in buffer layers on solar cells [4].

ALD is a vacuum-based method that allows precise control of coating composition and thickness even on convoluted surfaces. It differs from conventional chemical vapour deposition (CVD) by using alternate exposure of precursors that react exclusively with surface functional groups. Unlike CVD, where film growth is flux dependent, ALD film growth is mediated by surface exchange reactions. Sequential pulsing of reactants, interposed with a purge pulse of inert gas (N_2 or Ar), removes excess reactant and eliminates any vapor phase reactions. This results in only chemisorbed species remaining on the surface. A typical reaction sequence comprises a dose of metal alkoxide or covalent halide precursor, which saturates the surface with a (sub) monolayer of reactive compound. A second precursor such as water undergoes nucleophilic exchange with these surface ligands to grow the film in a layer by layer process. Growth rates of atomic

* E-mail address: gerry.triani@ansto.gov.au; tel: 61-2-9717-9070; fax: 61-2-9717-9630

Advances in Thin-Film Coatings for Optical Applications II, edited by Michael L. Fulton, Jennifer D. T. Kruschwitz,
Proc. of SPIE Vol. 5870, 587009, (2005) · 0277-786X/05/$15 · doi: 10.1117/12.638039

layer deposited films are typically sub-monolayer per cycle equating to 100-300 nm/h. Although slow growth rates are an inherent drawback of ALD processing, there are novel precursor chemistries [5] and strategies [6-7] that offer enhanced film growth rates.

Under optimised process conditions, ALD film growth is considered to be self-limiting, where film thickness varies linearly with the number of deposition cycles. This phenomenon typically falls within a narrow temperature window [1]. Outside of these boundary conditions, growth rates at higher temperatures have been reported to be influenced by desorption or decomposition of reactants. At deposition temperatures <150°C reduced reaction rates and physi-sorption influence film growth.

Thin-film dielectric materials are used extensively in optics as filters [8], mirrors [9] and for anti-reflection [10]. Typically, coatings used for optical interference require multi-layer structures. Accurate thickness control of alternating layers is paramount to ensure the desired performance. Although physical vapour deposition (PVD) methods such as reactive ion beam evaporation and cathodic sputtering, and chemical vapour deposition (CVD) processing are common technologies for coating glass and polymeric substrates, the design of complex periodic structures with specific spectral performance and functionality requires better control of thickness, composition, interface/bulk structure and conformality, For such structures, ALD emerges as an ideal method for producing multi-layered coatings with controlled nanostructure. Indeed, ALD multi-layer optical films have been reported by Riihela [11] using ZnS and Al_2O_3, deposited on soda glass at 500°C, using simple layered structures for antireflection, and on complex periodic configurations such as a Fabry-Perot filter. In another ALD study by Zaitsu[12] , the refractive index of a multilayer stack was adjusted by ALD using alternate TiO_2 and Al_2O_3 films deposited at 200°C. By varying the thickness of the high refractive index, titania layer and keeping the low index alumina film thickness constant, a composite film structure was prepared with an effective graded refractive index varying from 2.39 to 1.61.

The substitution of glass with transparent engineering polymer substrates, in applications such as display windows on portable electronic devices, has prompted the development of low temperature optical coatings [13-14]. In addition to specific optical functions, surface coatings on polymers are also being used to modify the physical properties (i.e. hardness and scratch resistance) of the softer substrate [15]. The deposition of ALD multi-layered coatings on glass substrates has been reported at high temperatures, however the deposition of dielectric layers at temperatures compatible with polymeric substrates has not been well documented. This paper reports on ALD grown films, of both titania and alumina, as discrete single films and as multiple layers on silicon, soda glass and polycarbonate at temperatures of between 100 and 200°C. In this temperature range, all films are amorphous. Atomic layer deposited thin-films were characterised using a suite of complimentary techniques to investigate the chemical homogeneity, interfacial/bulk structure and optical properties.

2. EXPERIMENTAL

Thin-films of alumina and titania were grown on silicon <100>, polycarbonate (Lexan®) and soda glass substrates using a flow-type hot-walled F-120 reactor from ASM Microchemistry. Substrates were positioned in the hot-zone of the vacuum chamber so the precursors coated both surfaces simultaneously. The reaction chamber was maintained at 1 mbar and deposition took place after an equilibrium temperature was achieved. Precursor vapour, from trimethyl aluminium (TMA), titanium tetrachloride ($TiCl_4$) and water was delivered from Peltier cooled reservoirs maintained at 20°C. For deposition within the ALD temperature window (i.e. 200-400°C), the dosing scheme for TiO_2 films was 0.3 seconds exposure by $TiCl_4$ followed by 0.5 seconds purge with N_2. The second reactant, H_2O was pulsed for 0.4 seconds followed by a 0.5 second N_2 purge pulse. Al_2O_3 films were grown under slightly different dosing conditions, a 0.4 second pulse of TMA followed by 0.5 second N_2 purge, followed by an equivalent H_2O pulse. Below 150 °C, the precursor pulse and purge regimes were optimised to ensure uniform film coverage by extending the precursor delivery and purge times. [16]

Multi-layered films, of alternating high and low refractive index, including graded index films were prepared following growth rate determination by ellipsometry. Variable angle spectroscopic ellipsometry measurements were made using a Sopra GESP-5 instrument over a wavelength range of 250-850 nm at three angles of incidence. Fitting of

ellipsometric parameters tan ψ and cos Δ was made using the Sopra Winelli software. The thickness, and optical constants (refractive index and extinction coefficient) were derived from spectra by modeling with the Levenberg-Marquardt regression algorithm.

X-ray reflectometry (XRR) was used to probe the nanostructure and interfaces of ALD deposited thin-films normal to the surface. Single and multiple layer stacks were measured on silicon wafers rather than on soda glass and polymer substrates as these substrates were not sufficiently flat for XRR. XRR measurements were collected on an X-pert Pro diffractometer from PANalytical. Data were modeled using the Parratt32 refinement package with a linear background correction [17]. By refining a structural model and fitting observed reflectivity data, the thickness (d), electron density (ρ_{el}) and interfacial roughness (σ) between layers was determined.

The composition of the films was analysed by secondary ion mass spectrometry (SIMS), on a Cameca ims 5f. Depth profiling was performed using Cs^+ primary ion beam, rastered over an area of 250x250 μm^2. Secondary cesium cluster ions (MCs^+) from a ~55 μm central region of the sputtered crater were detected and recorded.

Thin-films on silicon were prepared for cross-sectional transmission electron microscopy (TEM) by bonding the coated surfaces of two wafers together. A cylindrical core was then ultrasonically machined from the interface, and this was bonded into a brass tube of 3 mm diameter. Thin discs were then cut from this tube, ground to 80 μm thickness, mechanically dimpled to ~30 μm thickness and finally ion beam milled to electron transparency using a Gatan precision ion polishing systems (PIPS™). Surface coated polycarbonate specimens were sectioned using an ultramicrotome (Leica Ultracut™ UCT) with a 35º diamond knife at room temperature. Thin 50 nm sections were collected onto copper grids with holey carbon supports and specimens were examined using a JEOL 2010F TEM operated at 200 kV. This instrument was fitted with an energy dispersive x-ray spectrometer (EDS) which permitted qualitative analysis. It was also fitted with a Gatan Imaging Filter (GIF) which permitted energy filtered imaging.

3. RESULTS AND DISCUSSION

3.1 Growth rate and film uniformity

The growth rates (nm/cycle) of Al_2O_3 and TiO_2 films deposited at temperatures of 100 and 200°C were determined by spectroscopic ellipsometry and are recorded as nm/hour in Table 1. As can seen from the data, and reported in the literature [11,18], growth rates of films on the various substrates studied are different, due to the inherent nature of this surface mediated process. Most importantly, it is the nature of the substrate surface chemistry, which initiates nucleation, and growth of a continuous film, and the subsequent evolution of the nanostructure [19]. This is particularly evident on a hydride-terminated silicon surface where there is an observed incubation period before the onset of linear film growth [20-21].

At temperatures suitable for deposition on polycarbonate, the pulsing conditions were varied to ensure uniform film growth in the flow reactor. Accordingly, the dosing profile of the reactants, for the deposition of Al_2O_3, was modified to ensure completion of surface exchange reactions. In all cases, the extended pulse and purge times decreased the effective deposition rate (nm/hr) of Al_2O_3. Conversely, the dosing profile of precursors for TiO_2 deposition did not require longer pulsing times, as determined by quartz crystal microbalance measurements. The deposition rate (nm/hr) for TiO_2 increases at lower temperature. This is attributed to the reaction of physi-adsorbed species, which results in the growth of lower density, thicker films.

Table 1: ALD growth rate (nm/hr) for dielectric materials on various substrates

Deposition temperature	Dielectric Film	Silicon	Soda Glass	Polycarbonate
100°C	Al_2O_3	46	42	25
	TiO_2	187	146	276
200°C	Al_2O_3	202	180	
	TiO_2	101	90	

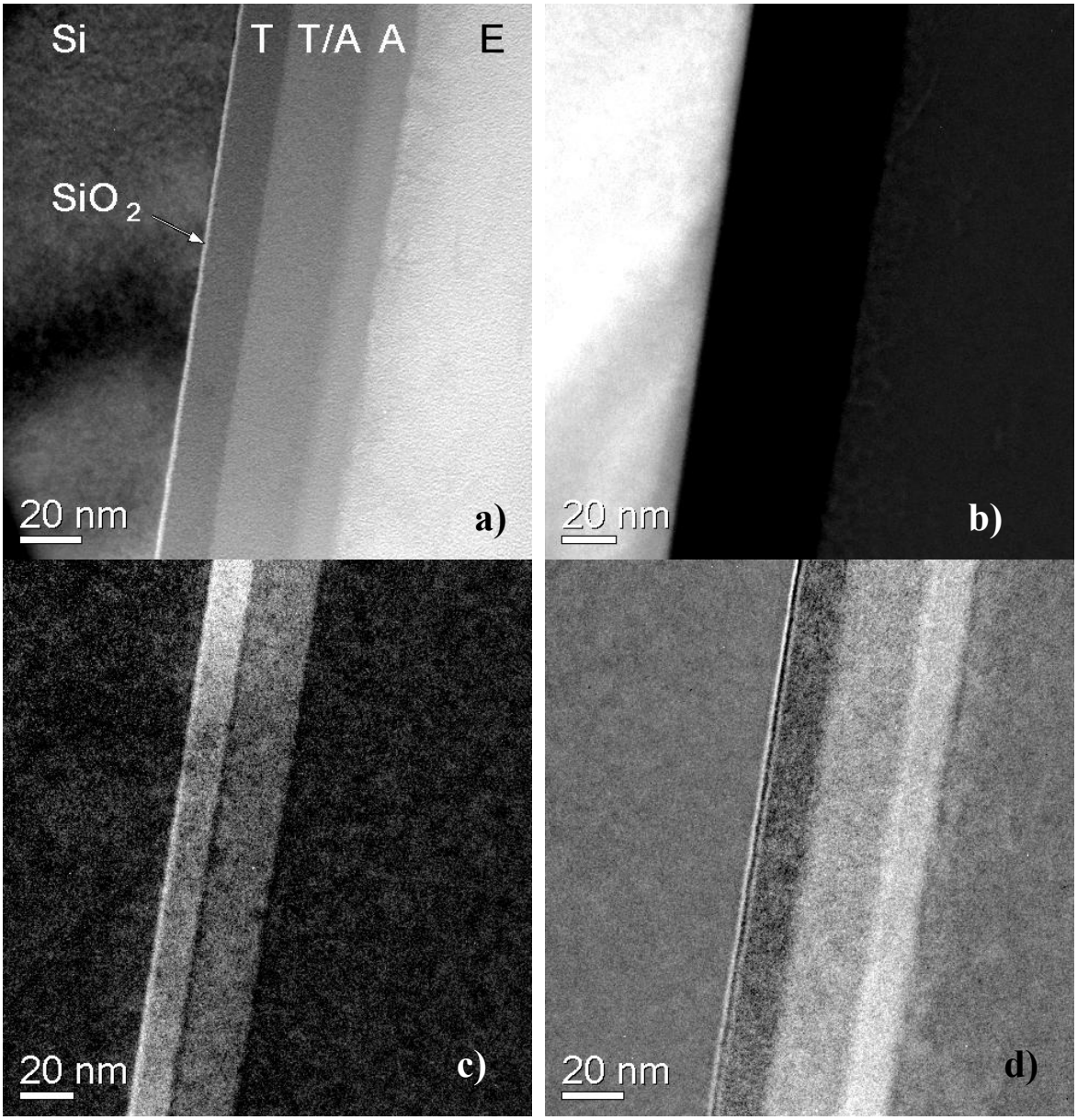

Figure 1: Energy filtered TEM images of the TiO_2/Al_2O_3 multi-layer film: a) Bright field image showing the silicon substrate (Si) and its native oxide layer (SiO_2). The three layers of the film are TiO_2 (T), an alloy of TiO_2 and Al_2O_3 (T/A) and Al_2O_3 (A). Epoxy (E) is from TEM specimen preparation. EFTEM maps are :b) Si $L_{2,3}$, c) Ti $L_{2,3}$, and d) Al $L_{2,3}$.

Figure 1 shows cross-sectional TEM images of a multilayered structure comprising a thin Al_2O_3 and TiO_2 film with a compositionally mixed alloy of the two dielectric materials as an intermediate layer on silicon. The silicon is on the left and a ~2 nm thick layer of native oxide (SiO_2) can be seen at the interface with the deposited film. The ALD film comprised three layers. The first layer (adjacent to the native oxide layer) was TiO_2 (T). This was 16.3 ± 0.4 nm thick. The greyscale intensity (Figure 1a) reflects the variation in mean atomic number between the layers. The middle layer is an alloy of TiO_2 and Al_2O_3 (T/A) 26.0 ± 0.5 nm thick, and the outer layer Al_2O_3 (A) 13.6 ± 0.7 nm thick. Epoxy (E) from TEM specimen preparation is present outside the Al_2O_3 layer.

In this present work, ALD deposition was used to produce amorphous multi-layers, which also include a stack with an alloy of Al_2O_3 and TiO_2. Since ALD film growth occurs at the sub-monolayer level, by alternating the precursor

sequence and frequency, it is possible to form intimately mixed oxide layers, with compositions that can be carefully controlled by varying the ratio of cycles of the two reactants. The disposition of the layers in Figure 1 was confirmed with energy filtered TEM (EFTEM). Images are constructed using characteristic electron energy loss signals caused by x-ray excitation of the film by the beam. EFTEM maps formed using the Si $L_{2,3}$ (Fig. 1b), Ti $L_{2,3}$ (Fig.1c) and Al $L_{2,3}$ (Fig.1d) energy loss signals revealed the elemental distributions for the respective elements. These images confirm the layers were discrete with chemically abrupt interfaces. The alloyed layer (T/A) in Fig. 1a showed the expected mixed composition, containing levels of Ti (Fig.1c) and Al (Fig.1d) intermediate to those of the corresponding layers of pure oxide.

The TEM images demonstrate the exceptional strength of ALD processing, in its ability to produce highly uniform layers, due to the self-limiting nature of the deposition process. The thickness of the individual layers is simply a function of the number of deposition cycles used with a particular precursor, before switching to a second reactant system. This approach has also been reported in a complementary study by Mitchell et al [22], who investigated nanolaminates with up to ten alternating layers of Al_2O_3 and TiO_2 where the target thickness was 20 nm. Conventional bright field imaging revealed the disposition of the layers on the basis of contrast differences, stemming from variations in mean atomic number. Several analysis modes were used to confirm thickness uniformity, including plasmon and energy filtered TEM and scanning TEM x-ray microanalysis. These techniques also showed that compositional homogeneity and thickness of the layers was maintained, regardless of the position within the stack.

3.2 Film density, surface roughness and refractive index

X-ray reflectometry provides information (thickness, density and roughness) about the films, complementary to that provided by TEM, but averaged over a substantially larger area (~cm^2). This technique probes the variation in electron density of the film normal to the surface with a resolution of a few nanometers. Figure 2 shows observed X-ray reflectivity data from single layers TiO_2 and Al_2O_3, a bi-layer and 5 tier multi-layer stack deposited on silicon at 200°C. The reflectivity curves have been divided by 10^2, 10^4 and 10^7 respectively, for clarity.

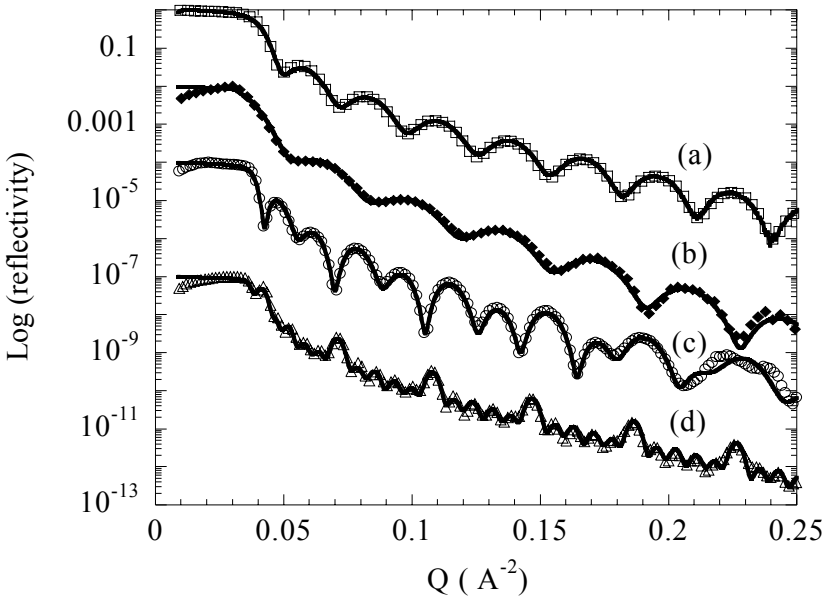

Figure 2: Observed (points) and calculated (solid lines) X-ray reflectivity profiles for (a) single TiO_2 (H) layer, (b) single Al_2O_3 (L) layer, (c) L/H bi-layer, (d) Five layer stack H/L/H/L/H/silicon . All films deposited at 200°C.

The points are the observed reflectivity data, while the solid lines represent the fit to these data from refined structural models. The results of the structural refinements are given in Table 2. Based on the fact that the fringe spacing (ΔQ_z) in reflectivity data is inversely proportional to film thickness ($\Delta Q_z \sim 2\pi/d$), a cursory examination of Figure 2 reveals that the Al_2O_3 monolayer film is thinner (16.8 nm) than the TiO_2 monolayer (21.2 nm). The closer fringes in the bi-layer and 5 layer systems indicate substantially thicker films. The beating pattern in these latter films is indicative of well-delineated multi-layer structures. The peaks in the 5 layer sample (repeating at ($\Delta Q_z \sim 0.04$ Å) are indicative of the (~15.5 nm) sub-structure; while the close-spaced fringes (repeating at($\Delta Q_z \sim 0.008$ Å) are due to the total film thickness (77.4 nm).

The density values in Table 2 are calculated from X-ray reflectometry data. The refined scattered length density ($Å^{-2}$) values assume stoichiometric Al_2O_3 and TiO_2 compositions. This table shows the density value (ρ) of the ALD TiO_2 films grown as single layers, a bi-layer and -5 tier multi-layer stack are approximately greater than 95 percent of the mass density for crystalline anatase 3.84 (g/cm^3). In contrast, the corresponding densities for ALD Al_2O_3 in Table 1 are significantly less than the reported values of 3.5-3.7 (g/cm^3) for bulk alumina [23]. In all cases, the calculated surface roughness (σ), is comparable to arithmetic mean R_a measured by atomic force microscopy. Growth temperature did not effect surface roughness of the deposited films in this study.

Table 2: Film density (ρ) and roughness (σ) of ALD Al_2O_3 and TiO_2 films at 200ºC

	TiO_2 (H)		Al_2O_3 (L)		(L/H) Bi-layer		(H/L/H/L/H) Stack	
	ρ (g/cm^3)	σ (nm)	ρ (g/cm^3)	σ (nm)	ρ (g/cm^3)	σ (nm)	ρ (g/cm^3)	σ (nm)
Si <100>	2.34	0.5	2.34	0.7	2.35	0.5	2.34	0.6
Layer 1	3.65	0.6	3.15	0.9	3.65	0.4	3.65	0.5
Layer 2					3.08	1.0	2.79	0.6
Layer 3							3.70	0.6
Layer 4							2.79	0.6
Layer 5							3.70	0.6

Figure 3 shows the film density (ρ) of single layer films deposited on silicon as a function of deposition temperature. These values were calculated from structural refinement of XRR data. The density of ALD films decreases at lower deposition temperatures. The values of ρ for ALD TiO_2 films are comparable to those reported by Laube et al [24], who compared the density of titania films prepared by several vacuum deposition techniques. In comparison, the densities of our ALD Al_2O_3 films are significantly lower than bulk α-alumina though they are similar to those reported previously by Groner [25].

The refractive index (n) of ALD films deposited as a function of temperature shows a similar trend to that of density. Films grown at lower temperature have higher porosity, which in turn affects the refractive index. Another trend observed is that n varies slightly with substrate, as summarised in Table 3. This is particularly evident in the deposition of TiO_2 films on polycarbonate at 100°C, which gives rise to thicker films but with lower n. This is attributed to the inclusion of competing physi-adsorbed species, that may not have completely reacted in the sub-second pulse/purge times.

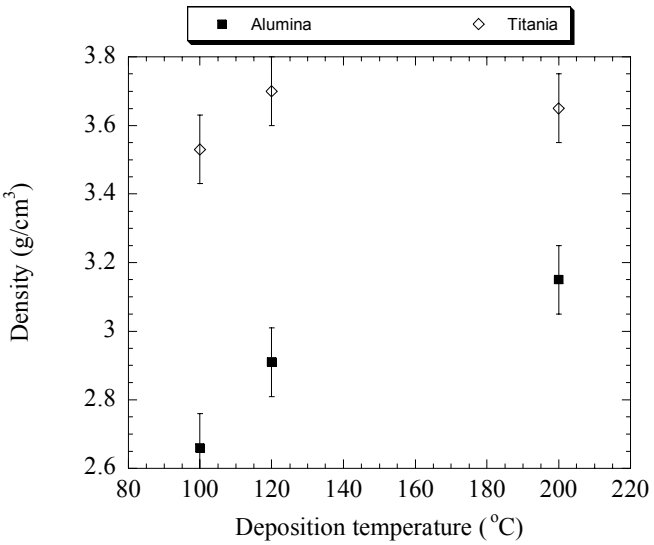

Figure 3: ALD Al_2O_3 and TiO_2 film density as a function of deposition temperature.

Table 3: Refractive index (λ =550 nm) of ALD TiO_2 and Al_2O_3 films grown on different substrates.

Deposition temperature	Dielectric Film	Silicon	Soda Glass	Polycarbonate
100°C	Al_2O_3	1.58	1.55	1.55
	TiO_2	2.36	2.36	2.30
200°C	Al_2O_3	1.58	1.58	
	TiO_2	2.42	2.42	

3.3 Chemical Homogeneity

SIMS analysis was used to investigate film composition as a function of depth. Figure 4 shows a typical SIMS depth profile of a multi-layer film with a compositional mixed layer, as presented in Figure 1. The outermost layer (0-500 s) is comprised of a homogeneous Al_2O_3 film. A relatively sharp interface occurs between the upper layer and the intermediate Al_2O_3/TiO_2 mixed layer (500-1500 s). An increase in chlorine content was detected in this intermediate layer. The interface between the intermediate layer and the lower TiO_2 layer (1500-1600 s) is less sharp, and is characterised by a gradual increase in Ti with an associated decrease in Al. This effect may be due to the presence of a mixed interfacial region that coincides with the addition of a third precursor (TMA) to form the alloy layer. Similar regions have not been observed at the interfaces between Al_2O_3 and TiO_2 layers in bi-layer structures (See Figure 5). The TiO_2 layer (1600-2000 s) has a distinct interface with the silicon substrate as evidenced by the sharp rise in the Si signal at 2000 s. The carbon content of the three layers was insignificant and as a consequence is not displayed.

Figure 5 illustrates a SIMS depth profile of a bi-layer film deposited at lower temperature. The depth profile demonstrates the relatively uniform nature of the upper Al_2O_3 (0-600 s) and the underlying TiO_2 layer (600-1200 s). The interfaces between the Al_2O_3 and TiO_2 layers (600 s) and the TiO_2 layer and the silicon substrate (1200 s) are both sharp. A titanium-oxide peak, of different Ti-O ratio to the film, is apparent at the Ti-Si interface (1200 s). This effect is qualitatively similar to that observed for most TiO_2 films on silicon. There is a small amount (4-8 at%) of residual chlorine in the TiO_2 layer at this temperature while the level of carbon is negligible.

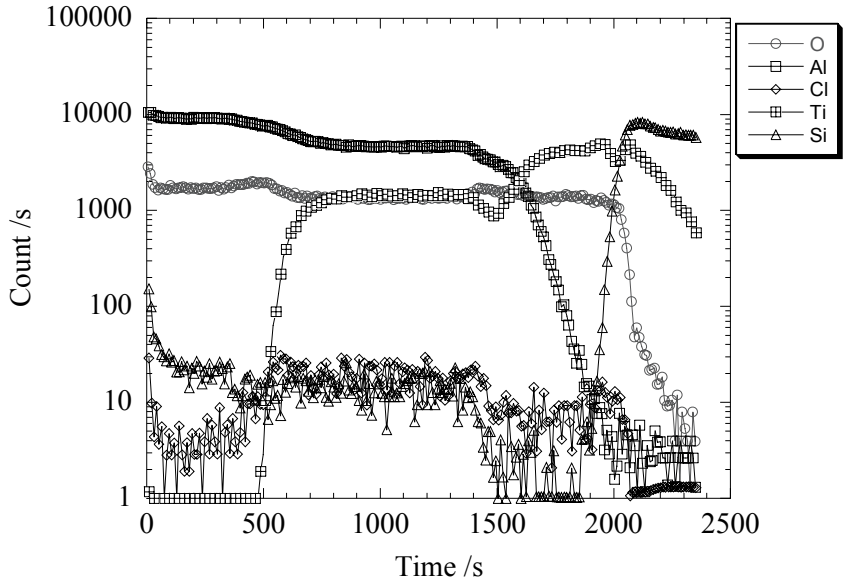

Figure 4: SIMS depth profile of an ALD Al_2O_3/TiO_2 multi-layer structure deposited at 200°C on silicon.

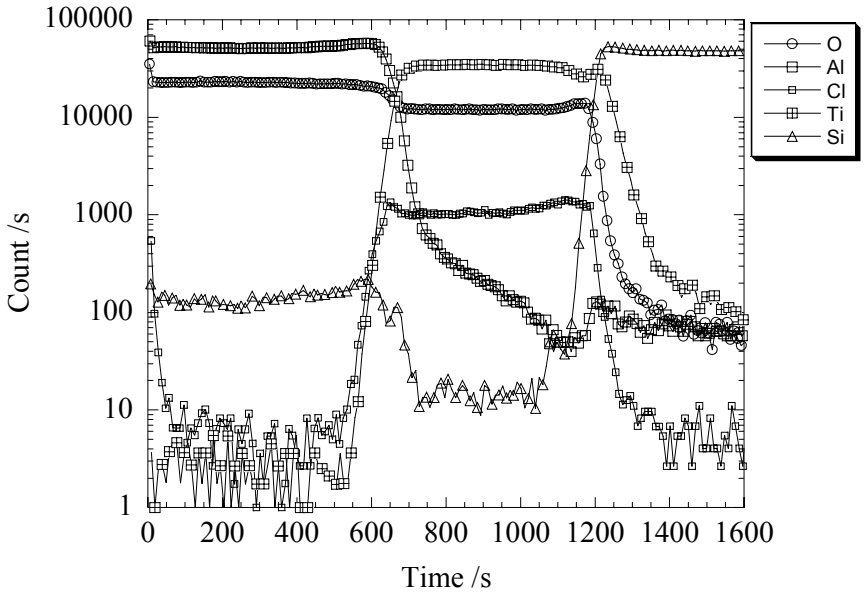

Figure 5: SIMS depth profile of ALD Al_2O_3/TiO_2 bi-layer deposited at low temperature on silicon.

3.4 Physical Properties of ALD films on Polycarbonate

The physical properties of ALD films on polycarbonate were examined on single and bi-layered structure with Al_2O_3 on the upper surface. Figure 6a shows a sectional cross-sectional TEM image of the bi-layer. Both layers are continuous and adherent. The hardness of the bi-layer structure and of the individual titania and alumina layers were determined from nano-indentation [26]. The hardness of ALD TiO_2 film was 5.5 GPa, while Al_2O_3 was 4.8 GPa. The hardness of the bi-layer structure was found to be 6 GPa. This is significantly higher than the hardness of the polycarbonate substrate which is only 0.13 GPa.

The impact damage response on polycarbonate was assessed by dropping a steel ball of approximately 16 mm diameter from a height of 1.27 m onto the centre of the sample (impact energy = 0.2 J). Figure 6(b) shows an optical image of the impact site with numerous short radial cracks in the film emanating from a region outside the contact area. No delamination of the film was observed indicating good adhesion. Recent tensile adhesion tests [26], of ALD films have shown that both single and bi-layer films display only minor de-bonding after pulling to about 10% strain, confirming the excellent interfacial adhesion.

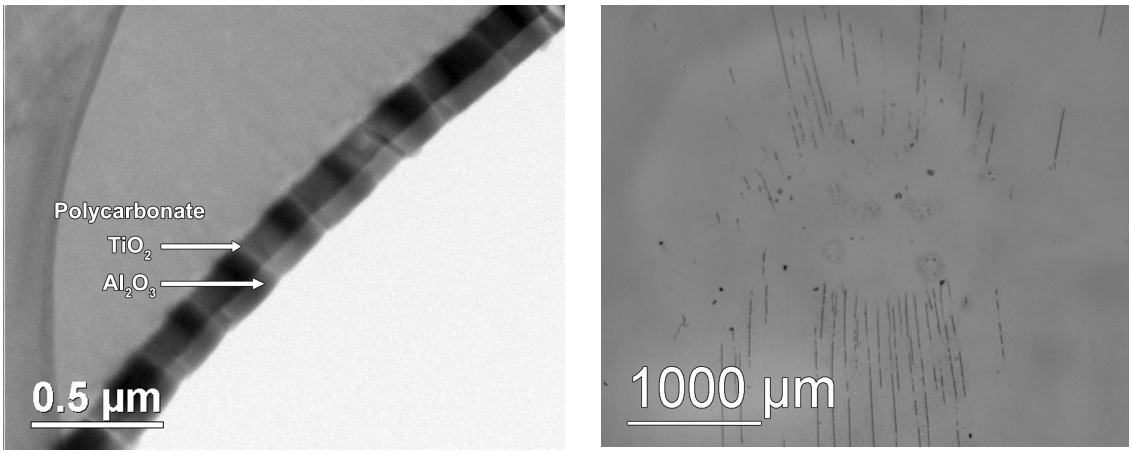

Fig. 6 a) Bright field cross-sectional TEM image of the Al_2O_3/TiO_2 bi-layer film deposited on polycarbonate . b) reflected optical image of the ALD film show cracks emanating from the impact zone.

4. CONCLUSION

Atomic layer deposition provides excellent control of thickness and chemical homogeneity for optical quality thin films over a temperature range 100-200 °C. Multi-layered structures with (a) alternating high and low refractive layers and (b) compositionally graded structures have been fabricated to demonstrate the versatility of this deposition method. Furthermore, this work has found that high quality ALD films can be deposited at low temperature on polymers.

From the suite of characterisation techniques, TEM and SIMS analysis show ALD films are uniform and chemically distinct with abrupt interfaces. XRR and ellipsometry were used to derive the film density and refractive index which, for the ALD films in this study, were lower than their equivalent bulk crystalline values. ALD coatings have also been shown to improve the mechanical performance of soft materials. This was clearly demonstrated by the significant increase in hardness observed for an ALD bi-layer film on polycarbonate.

In comparison to growth rates found in traditional vacuum deposition techniques, the growth rates of ALD dielectric materials such as Al_2O_3 and TiO_2 are rather low. Nevertheless, ALD has great potential in "bottom-up" fabrication of planar structures with excellent conformality. Beyond traditional multi-layer designs, ALD through its unique surface mediated reaction scheme can also provide a unique pathway for replication of complex two and three-dimensional structures, which are now being investigated for photonics [27].

ACKNOWLEDGEMENTS

The authors wish to thank colleagues of the Nano-Structural Engineering project for their support during the preparation of this paper.

REFERENCES

[1] T. Suntola, Mater Sci Rep. **4** (1989) 261.
[2] M. Kautzky, R. Lamberton, S. Chakravarty, L. Stearns, A. Kumar, and J. Dolejsi, AVS Topical Conference on Atomic Layer Deposition (2003).
[3] J.W. Erickson and J.W. Elam AVS 3rd International Conference on Microelectronics and Interfaces (2002) 42.
[4] F. Lenzmann M. Nanu, O. Kijatkina and A. Belaidi, Thin Solid Films, **451-452**, (2004) 639.
[5] L. Niinisto and M. Leskelä Thin Solid Films, **225** (1993) 130.
[6] M. Ritala, K. Kukli, A Rahtu, P Räisanen, M. Leskelä, T. Sajavaara and J Keinonen, Science. 288 (2000)319
[7] D. Hausmann, J. Becker, S. Wang and R.G. Gordon, Science. **298** (2002) 402.
[8] R.B. Sargent and N.A. O'Brien, MRS Bulletin **372** (2003)
[9] W.H. Southwell Opt Lett. **8** (1983) 584.
[10] H. Kumagai, K. Toyoda,K .Kobayashi,M. Obara and Y. Iimura App Phy Lett **70**, (1997) 2338.
[11] D. Riihelä, M. Ritala., R. Matero and M..Leskelä , Thin Solid Films, 289, (1996) 250.
[12] S. Zaitsu, T. Masahiro, M.Nakatsuka, T. Yamanaka and S. Motokoshi, App Phy Lett. **80** (2002) 2242.
[13] P. Munzert, U. Schulz and N. Kaiser, Surface and Coatings Tech, **174** (2003) 1048.
[14] M. Kuhr, S. Bauer, U. Rothhaar, D. Wolff Thin Solid Films, **442** (2003) 107.
[15] U. Schulz, U.B. Schallenberg, N Kaiser, App Optics, **41** (2002) 3107.
[16] G. Triani , P.J. Evans, K.S. Finnie, B.A. Latella, D.J. Attard, C.J. Barbe and J Bartlett, AVS Topical Conference on Atomic Layer Deposition (2003)
[17] L. G. Parratt, Phys. Rev. **95** (1954) 359
[18] M. Ritala, M. Leskelä, E. Nykanen, P. Soininen and L. Niinisto Thin Sold Films **225**, (1993) 288.
[19] K.S.Finnie, G. Triani, K.T. Short, D.R.G. Mitchell, D.J. Attard, J.R. Bartlett and C.J. Barbe, **440** Thin Solid Films, (2003) 109.
[20] E.P. Gusev, M Copel, E Cartier, I.J.R. Baumvol, C. Krug and M.A. Gribelyuk, Appl. Phy. Let **76** (2000) 176.
[21] M.M. Frank , Y.J. Chabal and G.D. Wilk Appl. Phy. Let. **82** (2003),4758.
[22] D.R.G.Mitchell, D.J. Attard, K.S. Finnie, G. Triani, C.J.Barbé, C. Depagne and J. Bartlett, **243** App. Surf. Sci. (2005) 265.
[23] CRC Handbook of Chemistry and Physics, 75th edn, R. Lide, (editor), CRC Press, Boca Raton (1994)
[24] M.Laube, F Rauch, C Ottermann, O Anderson and K Bange, Nucl. Instrum. Meth. **B 113** (1996) 288.
[25] M.D. Groner, F.H. Fabreguette, J.W. Elam, S.M. George, Chem. Mater. **16** (2004) 639.
[26] B.A. Latella, M Ignat and G.Triani, 4th Australian Congress on Applied Mechanics, (2005) 371.
[27] J.S.King, D Heineman, E. Graugnard and C.J.Summers, App Surf Sci. **244**(2005) 511.